

# The Discrete Wave Number Formulation of Boundary Integral Equations and Boundary Element Methods: A Review with Applications to the Simulation of Seismic Wave Propagation in Complex Geological Structures

MICHEL BOUCHON<sup>1</sup>

*Abstract*—We review the application of the discrete wave number method to problems of scattering of seismic waves formulated in terms of boundary integral equation and boundary element methods. The approach is based on the representation of the diffracting surfaces and interfaces of the medium by surface distributions of sources or by boundary source elements, the radiation from which is equivalent to the scattered wave field produced by the diffracting boundaries. The Green's functions are evaluated by the discrete wave number method, and the boundary conditions yield a linear system of equations. The inversion of this system allows the calculation of the full wave field in the medium. We investigate the accuracy of the method and we present applications to the simulation of surface seismic surveys, to the diffraction of elastic waves by fractures, to regional crustal wave propagation and to topographic scattering.

**Key words:** Seismic wave propagation, boundary integral equations, numerical simulation in elastodynamics, diffraction of elastic waves.

## *Introduction*

The propagation of seismic waves through complex geological structures can be studied by a variety of methods. The choice of the investigating technique depends in large part on the type of problem considered. When the propagating medium, for instance, is made up of relatively homogeneous layers separated by interfaces of arbitrary shape, or contains cracks or inclusions embedded in an otherwise relatively homogeneous geological formation, the use of boundary integral equations or boundary element methods is very appropriate. Several formulations of these methods in elastodynamics have been proposed over the last two decades. Here we shall focus our attention on the formulation based on the discrete wave number representation of the Green's functions. We shall review the approach and shall

---

<sup>1</sup> Laboratoire de Géophysique Interne et Tectonophysique, Université Joseph Fourier et Centre National de la Recherche Scientifique, BP 53X, 38041 Grenoble, France.

present new examples of applications which show the types and ranges of problems which can be investigated by this method.

### *Description of the Method*

Let us first consider the case, shown in Figure 1, of two homogeneous semi-infinite elastic half-spaces separated by an interface of arbitrary shape. For simplicity we begin with the two-dimensional antiplane problem. Let us assume that an elastic source is located in medium 1. Then, using Huygens principle, the elastic displacement wave field at a point  $P$  of medium 1 can be expressed in the form:

$$V(P) = V_0(P) + \int_S \sigma(Q) G(P, Q) dS(Q) \quad (1a)$$

where  $Q$  denotes a point of the interface  $S$ ,  $\sigma$  is an unknown source density function and  $G$  is the infinite space Green's function of medium 1. In writing equation (1a) we express the wave field at  $P$  as the sum of the direct source wave field  $V_0$  and of the diffracted wave field that we represent as the integral over the diffracting surface of an unknown source density function  $\sigma(Q)$  (each point of the interface acts as a source of radiation) times a term,  $G(P, Q)$ , which expresses the radiation produced at the observation point  $P$  by a unit force located at the interface point  $Q$ .

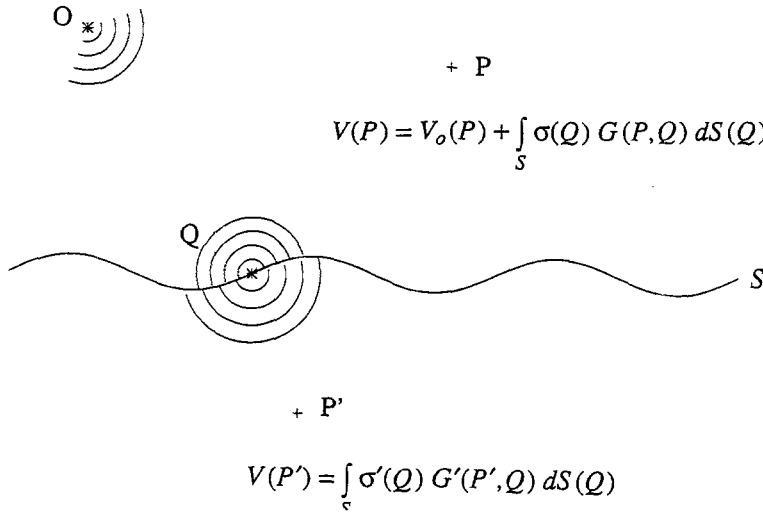


Figure 1  
Illustration of the method.

At an observation point  $P'$  of medium 2, we obtain in a similar way:

$$V(P') = \int_S \sigma'(Q)G'(P', Q) dS(Q) \tag{1b}$$

where  $G'$  is the infinite space Green's function for medium 2, and  $\sigma'$  is the unknown source density function representing the diffraction sources in medium 2.

A simple way to evaluate equations (1) is to assume that the source-medium configuration has a spatial periodicity  $L$  along a direction  $x$ , and to use the discrete wave number representation of the Green's functions (BOUCHON and AKI, 1977). For most applications  $x$  is the horizontal direction and will be referred as such in the following. This representation of the Green's functions, in the frequency domain  $\omega$ , by discrete horizontal wave number summation results from the spatial periodicity and may be written:

$$G(P, Q) = \sum_{m=-\infty}^{\infty} g(k_m, \omega, z_P - z_Q) e^{-ik_m(x_P - x_Q)} \tag{2}$$

where  $z$  is such that  $(x, z)$  defines a Cartesian coordinate system,  $g$  denotes the  $m$ th component of the plane wave expansion of the Green's function and where

$$k_m = \frac{2\pi}{L} m.$$

Then, discretizing the interface at equal  $\Delta x = L/N$  interval, where  $N$  is chosen to be an odd integer, equations (1) may be written simply:

$$\begin{aligned} V(P) &= V_0(P) + \sum_{i=1}^N \sigma_i \sum_{m=-N/2}^{N/2} g(k_m, \omega, z_P - z_i) e^{-ik_m(x_P - x_i)} \\ V(P') &= \sum_{i=1}^N \sigma'_i \sum_{m=-N/2}^{N/2} g'(k_m, \omega, z_{P'} - z_i) e^{-ik_m(x_{P'} - x_i)}. \end{aligned} \tag{3}$$

The limited range of the wave number summation in equation (3) results from the discretization of the interface at constant  $\Delta x$  interval. This spatial discretization implies a periodicity in the horizontal wave number space, just as the spatial periodicity of the interface shape implies a discretization in the horizontal wave number domain. Then choosing  $P$  and  $P'$  to be one of the discretized points  $Q_j$  of the interface, we obtain:

$$\begin{aligned} V(Q_j) &= V_0(Q_j) + \sum_{i=1}^N \sigma_i \sum_{m=-N/2}^{N/2} g(k_m, \omega, z_j - z_i) e^{-ik_m(x_j - x_i)} \\ V(Q_j) &= \sum_{i=1}^N \sigma'_i \sum_{m=-N/2}^{N/2} g'(k_m, \omega, z_j - z_i) e^{-ik_m(x_j - x_i)}. \end{aligned} \tag{4}$$

The continuity of the displacement wave field across the interface requires the equality of the two right hand sides of equations (4) and provides a system of  $N$

equations (as  $j = 1, N$ ) where the unknowns are the  $\sigma_i$  and the  $\sigma'_i$ . The continuity of the stresses across  $S$  provides  $N$  more equations and thus leads to a system of  $2N$  equations for  $2N$  unknowns. The solution of this system of linear equations yields the source density functions from which the wave fields can be evaluated throughout the medium. The time domain solution is obtained by Fourier transform. The unwanted effects of the periodicity are eliminated by performing the Fourier transform in the complex frequency plane.

The detailed formulation of the method for the antiplane (SH) case can be found in BOUCHON (1985) and CAMPILLO and BOUCHON (1985), and various applications have been presented in multilayered media for seismic exploration problems (CAMPILLO, 1987a; PAUL and CAMPILLO, 1988; BOUCHON *et al.*, 1989; HAARTSEN *et al.*, 1994), crustal wave propagation studies (CAMPILLO, 1987b; CAMPILLO *et al.*, 1993; CHAZALON *et al.*, 1993; GIBSON and CAMPILLO, 1994; PAUL, 1994; SHAPIRO *et al.*, 1996; PAUL *et al.*, 1996) and seismic risk evaluation (CAMPILLO *et al.*, 1988).

The presence of a flat free surface or of flat interfaces can be taken into account by replacing the infinite space Green's functions by the corresponding half-space or flat layered medium Green's functions. The  $g(k_m, \omega, z_P - z_Q)$  terms in equation (2), then include the free surface reflections or the layer reverberations in the form of reflectivity and transmissivity matrices (KENNETT, 1974; MÜLLER, 1985).

The corresponding equations for the  $P - SV$  case are presented in GAFFET and BOUCHON (1989, 1991), and they have been applied to study the effects of local geological structures on near-field and teleseismic source radiation (GAFFET *et al.*, 1994; GAFFET, 1995).

The above formulation is applicable as well to cases in which the diffracting surface is close, for instance to study the diffraction of seismic waves by cracks, cavities, or inclusions (BOUCHON, 1987; COUTANT, 1989).

This approach has also been used to simulate full wave form acoustic logging in an irregular borehole with axisymmetry (BOUCHON and SCHMITT, 1989). In this case, the borehole wall is the diffracting boundary between the acoustic borehole fluid and the elastic geological formation, and the Green's functions are expressed as discrete vertical wave number summations (CHENG and TOKSÖZ, 1981).

The applicability of the method described above requires that the medium surface and interfaces can be discretized at a constant spatial interval, along the direction of periodicity of the structure. This, however, may not always be convenient or possible. Such a case arises for instance when a diffracting boundary is perpendicular to the logical direction of periodicity of the structure (for instance, the presence of a vertical fault in an otherwise nearly horizontally layered medium). In this case, starting again with equations (1), we discretize the surface  $S$  into  $N$  surface elements  $\Delta S_i$  on which the source density functions  $\sigma$  and  $\sigma'$  are assumed to be constant. Equations (1) thus become:

$$\begin{aligned}
 V(P) &= V_0(P) + \sum_{i=1}^N \sigma_i \int_{\Delta S_i} G(P, Q) dS(Q) \\
 V(P') &= \sum_{i=1}^N \sigma'_i \int_{\Delta S_i} G'(P', Q) ds(Q).
 \end{aligned}
 \tag{5}$$

To calculate the Green's function integrals, we again use the discrete wave number representation for the Green's function (equation (2)). We then get the expression:

$$\bar{G}_{P,i} = \int_{\Delta S_i} G(P, Q) dS(Q) = \sum_{m=-M}^M h(k_m, \omega) \int_{\Delta S_i} e^{-i\gamma_m |z_P - z_Q|} e^{-ik_m(x_P - x_Q)} dS(Q)
 \tag{6}$$

and similarly for  $G'$ , where we have used the relations:

$$\begin{aligned}
 g(k_m, \omega, z_P - z_Q) &= h(k_m, \omega) e^{-i\gamma_m |z_P - z_Q|} \\
 \gamma_m &= \left[ \left( \frac{\omega}{\beta} \right)^2 - k_m^2 \right]^{1/2}, \quad \text{Im}(\gamma_m) \leq 0,
 \end{aligned}$$

and where  $\beta$  denotes the shear-wave velocity of medium 1, and  $M$  is an integer large enough to insure the convergence of the series.

The integration in equation (6) is performed analytically after approximating each surface element  $\Delta S_i$  by a segment of line. Next, choosing points  $P$  and  $P'$  as the middle  $Q_j$  of the  $j$ th surface element, one obtains:

$$\begin{aligned}
 V(Q_j) &= V_0(Q_j) + \sum_{i=1}^N \sigma_i \bar{G}_{j,i} \\
 V(Q_j) &= \sum_{i=1}^N \sigma'_i \bar{G}'_{j,i}.
 \end{aligned}
 \tag{7}$$

Similar to equations (4), the continuity of the displacement wave field across the interface requires the equality of the two right-hand sides of equations (7) and provides a system of  $N$  equations (as  $j = 1, N$ ) where the unknowns are the  $\sigma_i$  and the  $\sigma'_i$ . The continuity of the stresses across  $S$  provides  $N$  more equations and thus leads to a system of  $2N$  equations for  $2N$  unknowns. The inversion of the system and the Fourier transform of the resulting solution yield, as previously, the time domain elastic wave field throughout the medium.

The integration scheme of the discrete wave number Green's functions over boundary elements was first proposed by KAWASE (1988). His boundary element formulation, however, is based on the elastodynamic representation theorem in which the unknowns are the displacement and stresses on the boundaries (an approach usually referred to as the direct boundary element method). In the formulation described above, the problem is set up in terms of Huygens principle of diffraction, and the unknowns are the strengths and phases of the surface diffracting

sources. A discussion of the relation between the two approaches may be found in COUTANT (1989). Applications of the direct boundary element discrete wave number method to observations of ground shaking during earthquakes are presented in KAWASE and AKI (1989, 1990).

A more complete presentation of the boundary element formulation described above can be found in BOUCHON and COUTANT (1994). This approach has also been applied to the calculation of the radiation from a point source located in a fluid-filled borehole embedded in a flat layered geological formation (BOUCHON, 1993; DONG *et al.*, 1995). In this case the borehole wall is the diffracting surface between the borehole fluid and the layered formation. The Green's functions are then expressed as discrete radial wave number summations (BOUCHON, 1981) and are integrated analytically over the cylindrical elements of the borehole wall.

The generalization of the method to the three-dimensional case is straightforward. The source-medium configuration is then assumed to be periodic in the two horizontal ( $x$  and  $y$ ) directions, and the Green's functions (equation (2)) are expressed as double summations over the  $x$  and  $y$  components of the wave number (BOUCHON, 1979). The corresponding equations relative to an irregular 3D topography can be found in BOUCHON *et al.* (1996).

One limitation inherent to boundary integral equation or boundary element methods is the size of the system of equations which must be solved when the medium is complex or when the distance range of propagation is large compared to the considered wavelengths. The number of equations of the system is equal to the number of discretized points (or elements) representing the diffracting surfaces and interfaces times the number of boundary conditions which must be matched. The discretization is done automatically for each frequency: At low frequencies, a minimum number of points is assumed for each surface or interface, insuring that the geometry of the diffracting boundaries is well defined; at higher frequencies, the discretization interval is usually chosen to be about one third of the shortest wavelength present in the two media surrounding the interface. At high frequencies, the number of equations may thus become very large. Ways to drastically reduce the size of this system have been investigated and are presented in BOUCHON *et al.* (1995).

### *Tests of Accuracy of the Method*

The first test of accuracy of the method is illustrated in Figure 2. An explosive source is located at the surface of a flat layered half-space and the vertical displacement is recorded along a surface profile. The source pressure time dependence is a Ricker wavelet with a center frequency of 50 Hz. Only the downgoing wave field radiated by the explosion is considered here (that is, the direct arrivals at the receivers have been removed) in order to emphasize the reflected and

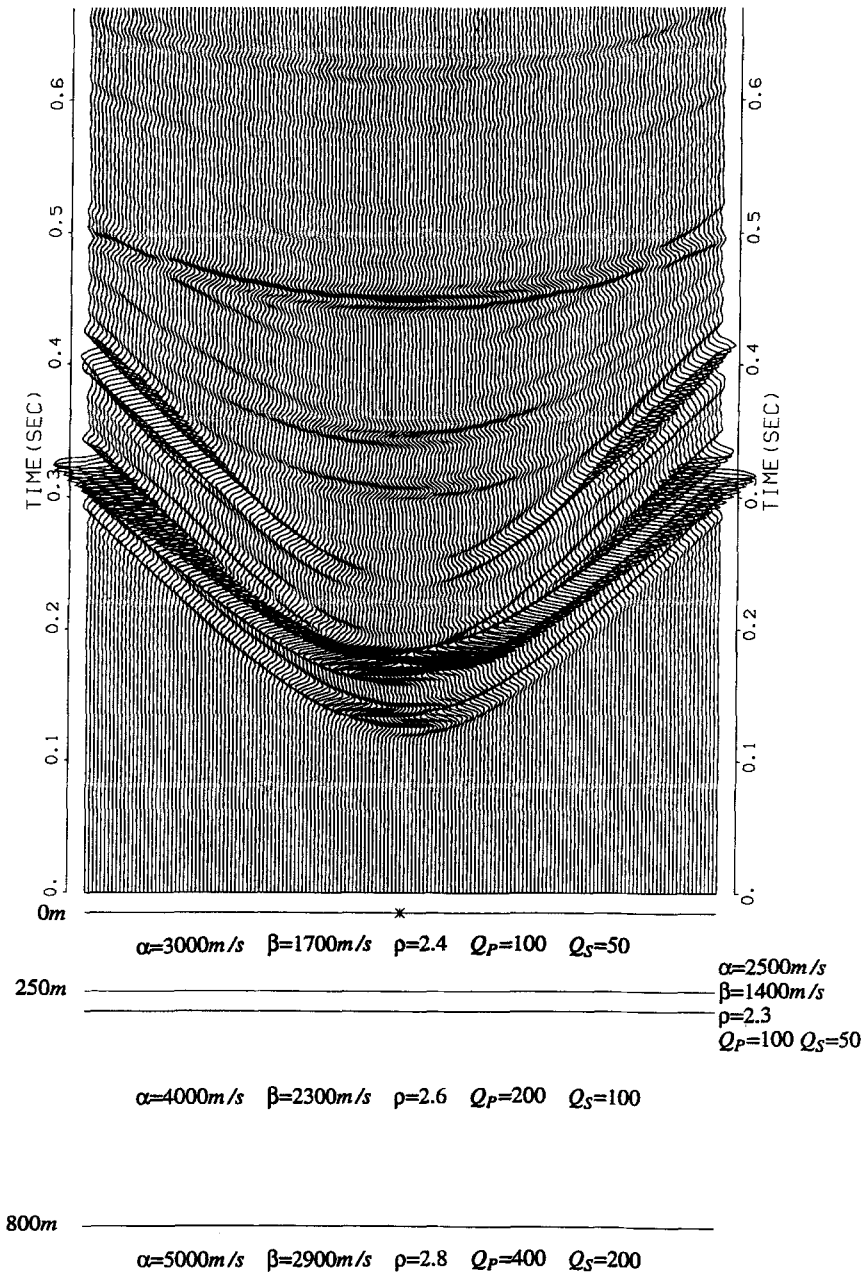


Figure 2

Comparison of the vertical displacement traces obtained using the boundary integral equation formulation with the flat layers solution for the configuration shown at the bottom of the figure. The star indicates the location of the explosive source. The direct wave field has been removed from the solutions.

diffracted arrivals. The explosive source radiation is expressed by its discrete wave number representation in a way similar to equation (2). Two traces are superposed at each receiver. One is calculated by the boundary integral equation/discrete wave number method: the surface and the three interfaces are discretized at equal spatial interval along the horizontal direction, and diffracting sources are applied at each discretized point. The other trace is calculated by using the discrete wave number method for flat layered media (BOUCHON and AKI, 1977): each wave number component of the explosive source radiation is combined with the reflectivity and transmissivity propagator matrices (KENNETT, 1974), which include the explicit expressions of the reflection and transmission coefficients of the plane waves at plane interfaces.

The second test of accuracy of the method is taken from a study of the diffraction of elastic waves by a crack (BOUCHON, 1987). The particular configuration involves a  $P$  wave normally incident on a Griffith crack located in an infinite elastic medium. Following MAL (1970), we calculated the crack opening for various wavelengths of excitation. Our results are compared to his solution in Figure 3. In

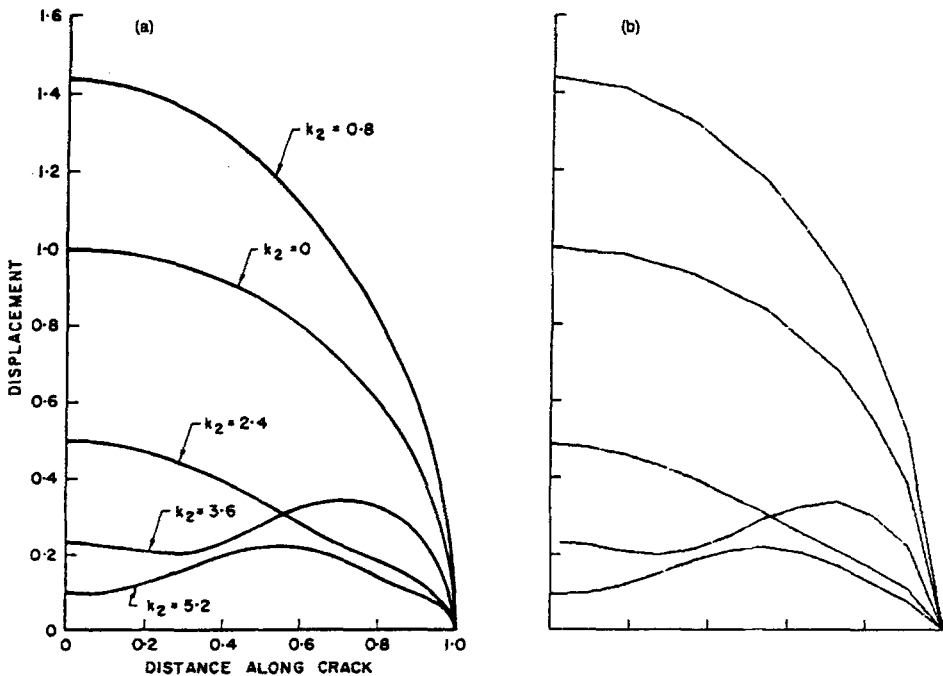


Figure 3

(a) Amplitude of the displacement of the face of a Griffith crack calculated by MAL (1970) for a vertically incident  $P$  wave for various frequencies of excitation. The results are normalized to the static displacement at the center of the crack.  $k_2$  denotes the shear wave number. (b) The same as (a) calculated using the method described in the text. (After BOUCHON, 1987)



our model the crack contour is represented by 42 points (21 points for each face of the crack), and the periodicity length, chosen to be large enough for the effects of the neighboring cracks to be negligible, is 1023 times the discretization interval. The calculations presented include wavelengths as small as 1.05 times the crack length and are for a Poisson ratio of 0.25. The static solution was approximated by taking an incident wavelength equal to 100 times the crack length.

The third test addresses the case in which the diffracting surfaces are represented by boundary elements over which the Green's functions are integrated. The medium, shown in Figure 4a, consists of a flat layered crustal structure overlaying a mantle half-space. The source is a line of horizontal shear dislocation occurring on a vertical plane and located at 10 km depth. The receivers are placed along a linear profile which extends in a direction perpendicular to the line of dislocation. The time dependence of the dislocation is a smooth step function with a rise time of about half a second. Two calculations are made: For the first one we consider the problem as one involving a source embedded in a flat layered medium and employ the discrete wave number method coupled with the reflectivity and transmissivity matrices. For the second calculation we consider that we have two independent layered media separated by a fictitious vertical interface located 200 km from the source. We thus treat the problem as if the crustal-mantle structure on both sides of the 200 km mark was different. We divide the fictitious vertical boundary into surface elements. We calculate the mathematical expressions of the Green's functions  $G$  and  $G'$  for the crust-mantle structure applying the discrete wave number method. We analytically integrate the resulting expressions over each surface element (equation (6)). We finally invert the linear system of equations and obtain the two source distributions  $\sigma$  and  $\sigma'$ , from which we calculate the seismic ground velocity produced at the receivers. In carrying out this procedure we assume that the fictitious surface of separation between the two media extends from the free surface down to a finite depth (chosen as 45 km) below which little seismic energy is present.

The comparison between the two sets of results is displayed in Figure 4a. The frequency range considered extends from 0 Hz (static) to 4 Hz. The periodicity length  $L$  used in the discrete wave number method for the two calculations is 850 km. The agreement between the two solutions proves the validity of the approach. A similar comparison is presented in Figure 4b for the surface displacement. In this case a slight discrepancy exists between the very long period near-static displacement fields of the two solutions beyond 200 km. This is due to the limited extent in depth considered (45 km) for the theoretically semi-infinite diffracting boundary.

### *Examples of Simulation*

The first example of simulation is presented in Figure 5. The geological structure considered is an irregularly layered medium, with an irregular topography. The

surface and the three interfaces are discretized with an equal spatial interval along the horizontal direction, and diffracting sources are applied at each discretized point. The seismic source is a surface explosion with a pressure time dependence given by a Ricker wavelet centered around 50 Hz. Frequencies from 0 Hz to 100 Hz are included in the calculation. Only the downgoing wave field radiated by the explosion is considered here (that is, the direct arrivals at the receivers have been removed) in order to emphasize the reflected and diffracted arrivals. The resulting vertical displacement is recorded at an array of surface receivers. Figure 2 provides a comparison of these results with the case where the surface and the interfaces are flat.

The second example is taken from a study of diffraction of elastic waves by fluid-filled cracks conducted by COUTANT (1989), and is depicted in Figure 6. A

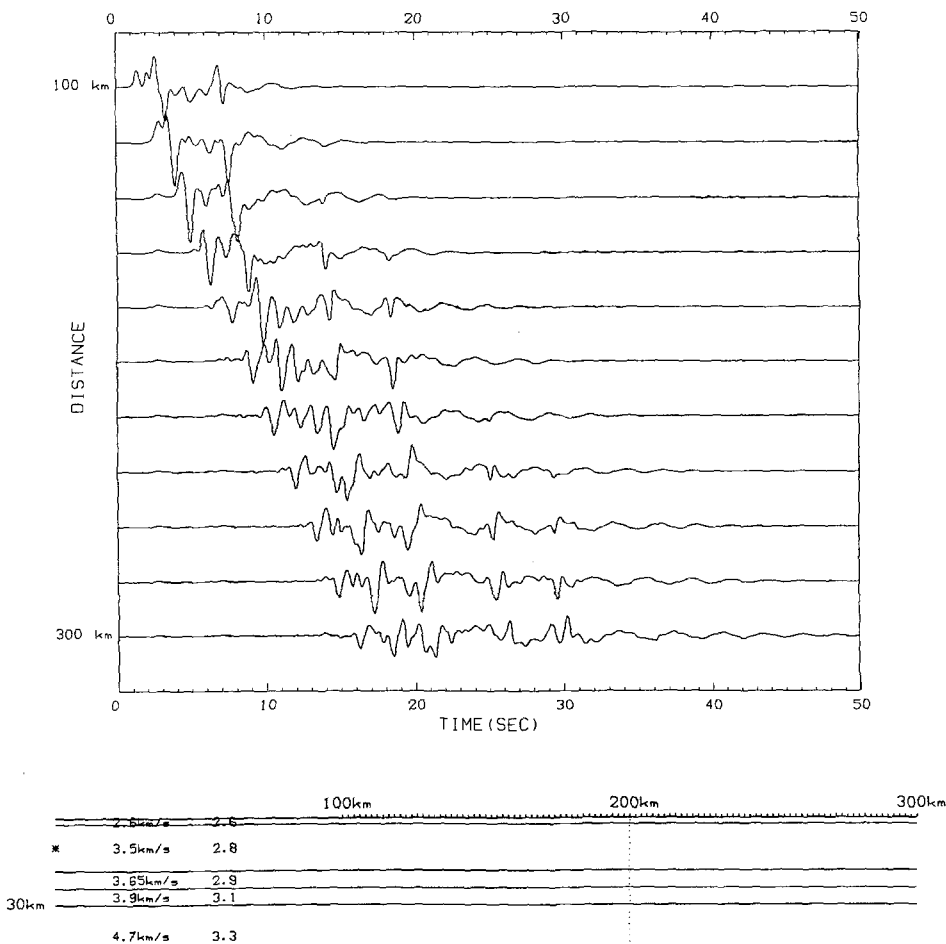


Figure 4 (a)

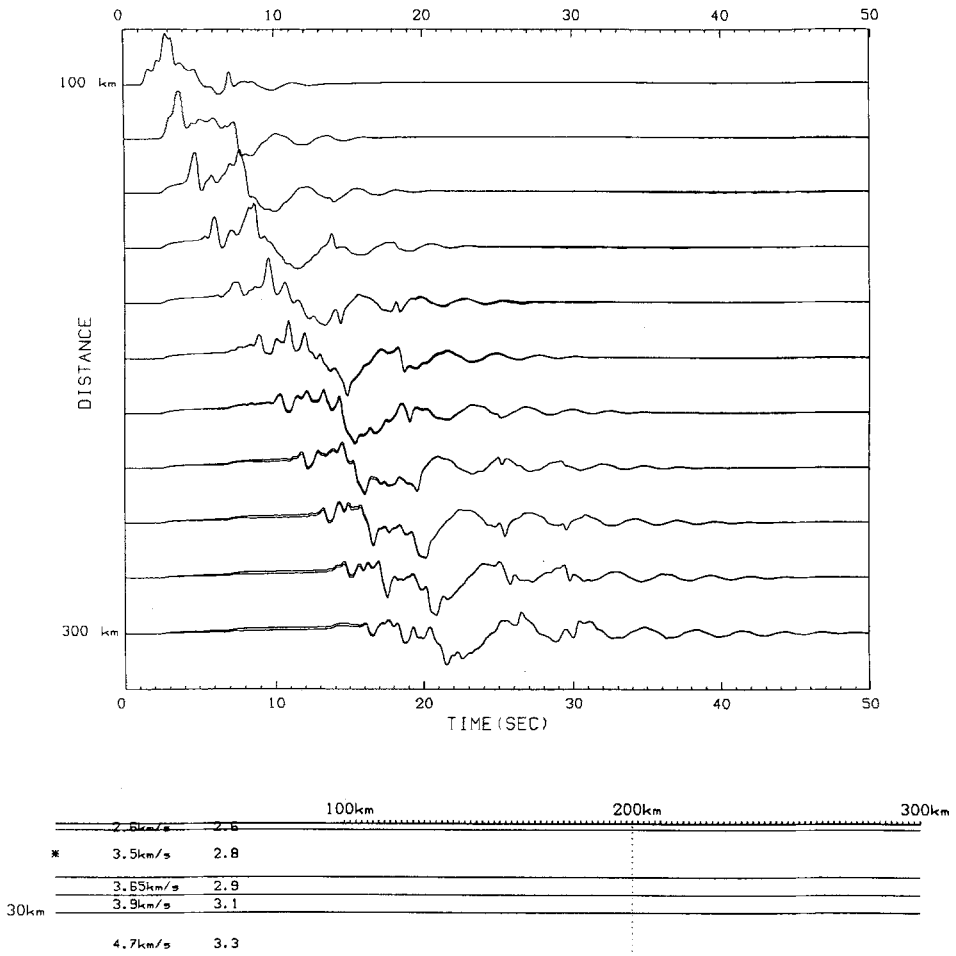


Figure 4(b)

(a) Comparison of the ground velocity traces obtained using boundary elements with the flat layers solution for the configuration depicted at the bottom of the figure. The star indicates the earthquake location. The time dependence of the dislocation is a smooth step function defined by:  $f(t) = [1 + \text{atan}(t/t_0)]/2$  with a rise time  $t_0$  equal to 0.5 s. The fictitious diffracting surface along which the sources are distributed is represented by the dotted line. A reduced time equal to the epicentral distance divided by the mantle shear wave velocity has been applied to the traces. (b) The same as (a) for the ground displacement.

plane S-wave pulse is incident on a fractured region embedded in an otherwise elastic homogeneous medium. The fractured area considered extends over 100 m in length and 3 m in width, and it is made up of 10 identical 20-m-long cracks with 2 mm thickness and filled with water. The compressional and shear-wave velocities and density of the elastic formation are respectively 3000 m/s, 1732 m/s and 2.69 g/cm<sup>3</sup>, while the compressional wave velocity and density of the fluid are 1090 m/s and 1.0 g/cm<sup>3</sup>. The source pulse is a Ricker wavelet with a 150 Hz central frequency. The receivers are placed around the cracks at a mean distance of 150 m. The

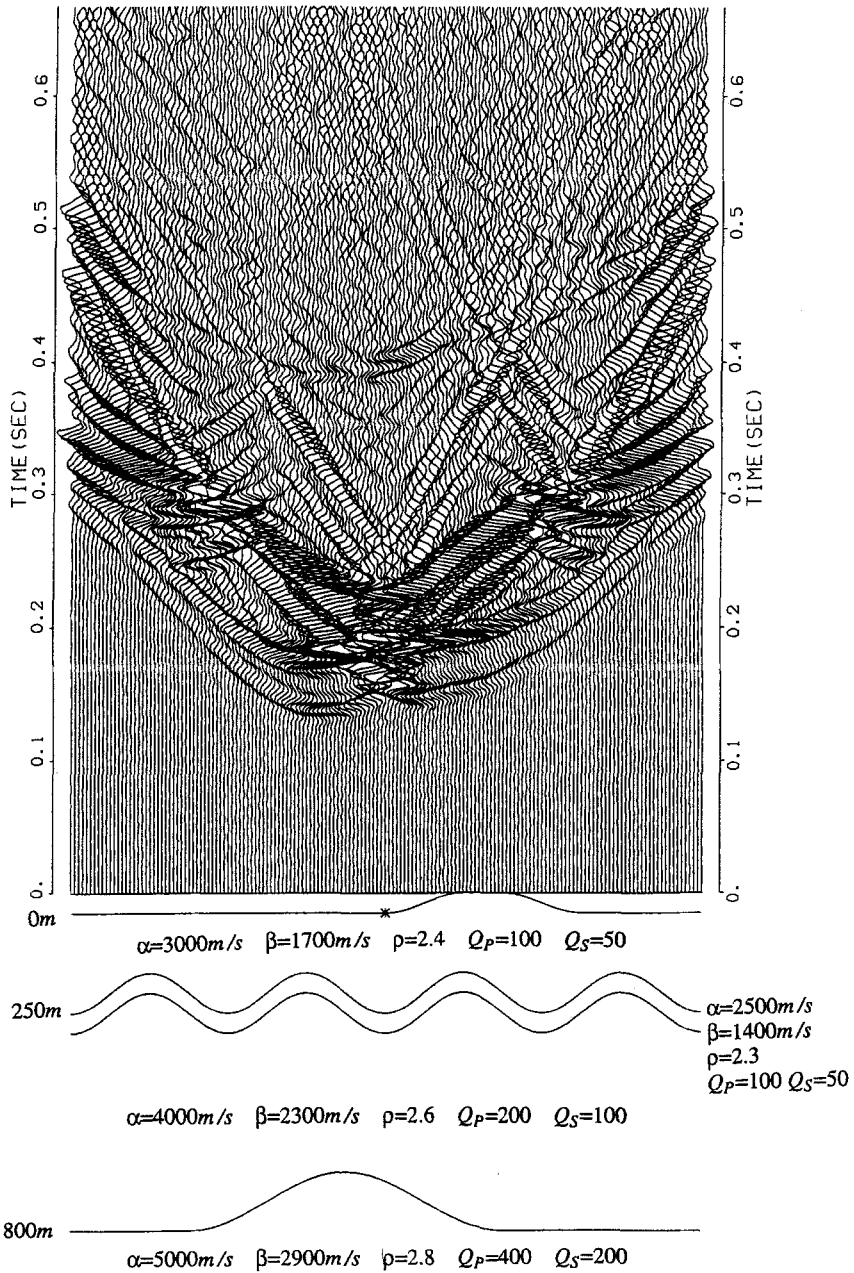


Figure 5

Simulation of a shallow surface seismic survey. The explosion location is indicated by a star. The traces show the vertical surface displacement. The direct wave field has been removed from the solution.

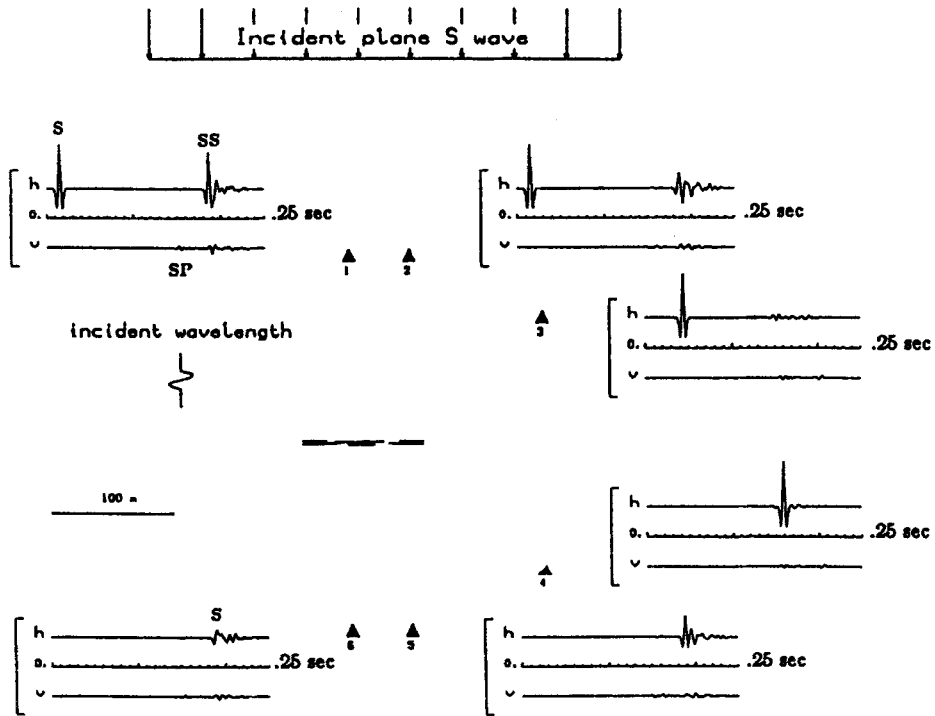


Figure 6

Simulation of the diffraction of an *S*-wave pulse by a fluid-filled fracture zone. The receiver locations are depicted by triangles. Displacements are shown for the horizontal *h* and vertical *v* components. (After COUTANT, 1989)

seismograms at stations 1, 2 and 3 display the incident (*S*) and the reflected (*SP* and *SS*) wave fields, while those at stations 4, 5 and 6 display the transmitted (*S*) wave field. The coda following the reflected and transmitted arrivals represents multiple scattering between the individual cracks.

For the third example, we use the boundary element formulation. The medium considered (Figure 7) is a layered crustal structure, except for the presence of a fault which affects the Moho and the lower crust. We define a diffracting boundary which follows the fault surface and separates the flat layered medium on the right-hand side of the fault from the one on the left-hand side of the fault. We truncate this boundary at a depth of 45 km, and we divide it into surface elements. We then calculate the expressions of the Green's functions for the two flat layered media, and integrate them over each surface element. We finally set up the linear system of equations which expresses the continuity of displacement and stress along the defined boundary, and we invert this system iteratively. The earthquake source is modeled as a line of horizontal shear dislocation occurring on a vertical plane at a depth of 10 km and is located about 200 km from the fault. The time dependence

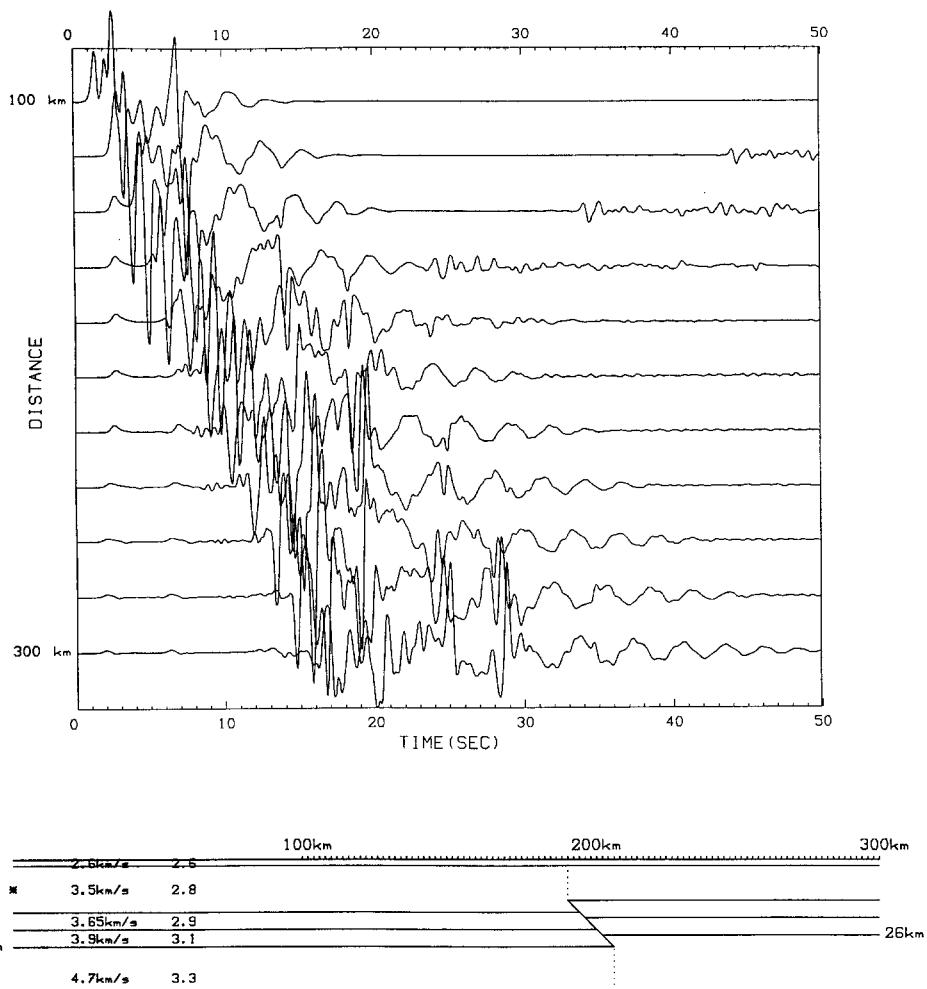


Figure 7

Simulation of the effect of a dipping fault in the lower crust on regional wave propagation. The earthquake location is indicated by a star. The boundary along which the diffracting source elements are distributed follows the fault and the dotted line. A reduced time equal to the epicentral distance divided by the mantle shear wave velocity has been applied to the traces.

of the dislocation is the same as the one used in Figure 4, and the frequency range extends from 0 Hz (static) to 4 Hz. The receivers are placed along a linear array perpendicular to the line dislocation and to the fault. The presence of a back scattered wave field originating from the fault is clearly seen. One may also observe a decrease in amplitude and a shift in arrival time of the refracted mantle shear wave at the crossing of the fault.

The final illustration of the method is the diffraction of an incident *P* wave by a three-dimensional topographic feature. The topography considered is a 100-m-

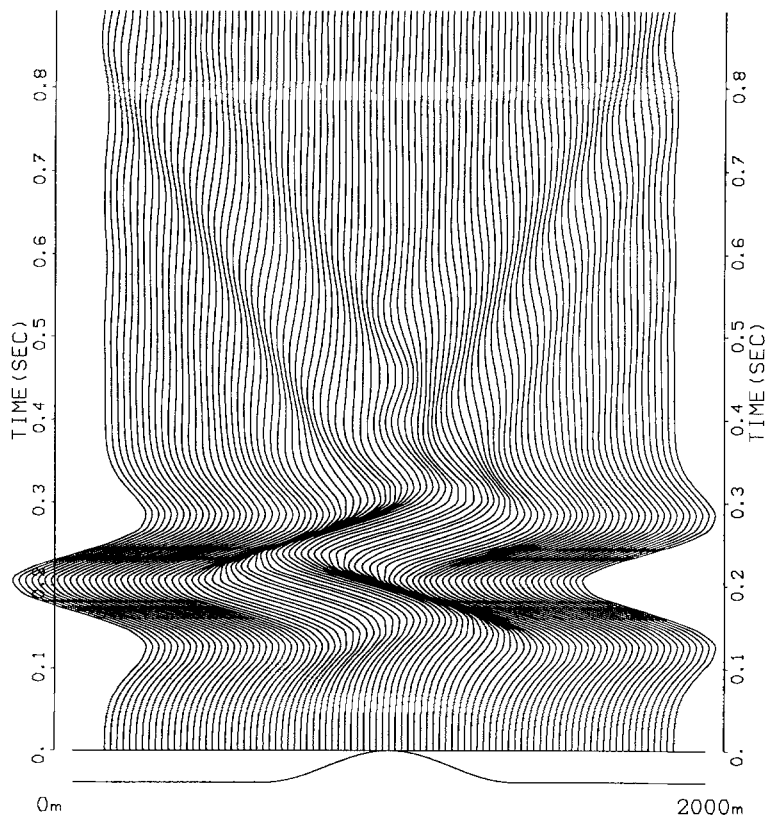


Figure 8

Simulation of the surface vertical displacement produced by a  $P$  wave vertically incident on a 3D hill topography. The calculation is made for a linear receiver profile crossing the top of the hill. The corresponding topographic profile is depicted.

high hill with a circular base of 400 m radius, and with cosine-shape flanks. The  $P$  wave velocity of the medium is 3000 m/s and the Poisson ratio is 0.25. The incident wave is a plane vertically incident Ricker-type pulse of 5 Hz central frequency. The surface is discretized into a two-dimensional array of points distributed at equal interval along two Cartesian horizontal directions  $x$  and  $y$ . Periodicity of the topography is assumed along these two directions for the frequency domain calculation, although its effect is not present in the time domain solution. For the present simulation, the periodicity length is 2000 m along both directions, and the number of discretized surface points is  $33 \times 33$  at low frequencies. At higher frequencies the discretization interval is chosen to be about one third of the shear-wave wavelength. The resulting vertical displacement calculated along a linear profile crossing the top of the hill is displayed in Figure 8. The major feature is the presence of a diffracted Rayleigh wave which is generated near the top of the hill.

### Conclusion

We have presented the application of the discrete wave number method to problems of scattering of seismic waves formulated in terms of boundary integral equation and boundary element methods. The approach is well suited when the medium comprises relatively homogeneous layers separated by interfaces of arbitrary shape, or contains cracks or inclusions embedded in an otherwise relatively homogeneous geological formation. We have reviewed the physical principles and the mathematical developments of the method, and we have demonstrated its accuracy by comparing the results with existing solutions for configurations in which such solutions are known. Fields of application of the method that we have investigated include the simulation of seismic exploration data, the study of regional seismic wave propagation in laterally-varying crustal structures and the diffraction of elastic waves by fractures and by 3D topography.

### Acknowledgments

I thank Keiiti Aki, Michel Campillo, Olivier Coutant, Stéphane Gaffet, Craig Schultz, Nafi Toksöz, Denis Schmitt, Wenjie Dong, Arthur Cheng, Matthijs Haartsen, and Hiroshi Kawase, whose work made this study possible.

### REFERENCES

- BOUCHON, M. (1979), *Discrete Wave Number Representation of Elastic Wave Fields in Three-space Dimensions*, J. Geophys. Res. **84**, 3609–3614.
- BOUCHON, M. (1981), *A Simple Method to Calculate Green's Functions for Elastic Layered Media*, Bull. Seismol. Soc. Am. **71**, 959–971.
- BOUCHON, M. (1985), *A simple Complete Numerical Solution to the Problem of Diffraction of SH Waves by an Irregular Surface*, J. Acoust. Soc. Am. **44**, 1–5.
- BOUCHON, M. (1987), *Diffraction of Elastic Waves by Cracks or Cavities Using the Discrete Wave Number Method*, J. Acoust. Soc. Am. **81**, 1671–1676.
- BOUCHON, M. (1993), *A Numerical Simulation of the Acoustic and Elastic Wave Fields Radiated by a Source in a Fluid-filled Borehole Embedded in a Layered Medium*, Geophysics **58**, 475–481.
- BOUCHON, M., and AKI, K. (1977), *Discrete Wave-number Representation of Seismic Source Wave Fields*, Bull. Seismol. Soc. Am. **67**, 259–277.
- BOUCHON, M., and SCHMITT, D. P. (1989), *Full-wave Acoustic Logging in an Irregular Borehole*, Geophysics **54**, 758–765.
- BOUCHON, M., CAMPILLO, M., and GAFFET, S. (1989), *A Boundary Integral Equation—Discrete Wave Number Representation Method to Study Wave Propagation in Multilayered Media Having Irregular Interfaces*, Geophysics **54**, 1134–1140.
- BOUCHON, M., and COUTANT, O. (1994), *Calculation of Synthetic Seismograms in a Laterally-varying Medium by the Boundary Element—Discrete Wave Number Method*, Bull. Seismol. Soc. Am. **84**, 1869–1881.
- BOUCHON, M., SCHULTZ, C. A., and TOKSÖZ, M. N. (1995), *A Fast Implementation of Boundary Integral Equation Methods to Calculate the Propagation of Seismic Waves in Laterally-varying Layered Media*, Bull. Seismol. Soc. Am. **85**, 1679–1687.



- BOUCHON, M., SCHULTZ, C. A., and TOKSÖZ, M. N. (1996), *Effect of 3D Topography on Seismic Motion*, J. Geophys. Res. 101, 5835–5846.
- CAMPILLO, M. (1987a), *Modeling of SH-wave Propagation in an Irregularly Layered Medium—Application to Seismic Profiles near a Dome*, Geophys. Prosp. 35, 236–249.
- CAMPILLO, M. (1987b), *Lg Wave Propagation in a Laterally Varying Crust and the Distribution of the Apparent Quality Factor in Central France*, J. Geophys. Res. 92, 12604–12614.
- CAMPILLO, M., and BOUCHON, M. (1985), *Synthetic SH-seismograms in a Laterally Varying Medium by the Discrete Wave Number Method*, Geophys. J. Roy. Astr. Soc. 83, 307–317.
- CAMPILLO, M., BARD, P. Y., NICOLLIN, F., and SANCHEZ-SESMA, F. (1988), *The Mexico Earthquake of September 19, 1985—The Incident Wave Field in Mexico City During the Great Michoacan Earthquake and its Interaction with the Deep Basin*, Earthq. Spectra 4, 591–608.
- CAMPILLO, M., FEIGNER, B., BOUCHON, M., and BÉTHOUX, N. (1993), *Attenuation of Crustal Waves across the Alpine Range*, J. Geophys. Res. 98, 1987–1996.
- CHAZALON, A., CAMPILLO, M., GIBSON, R. and CARRENO, E. (1993), *Crustal Wave propagation Anomaly across the Pyrenean Range. Comparison between Observation and Numerical Stimulations*, Geophys. J. Int. 115, 829–838.
- CHENG, C. H., and TOKSÖZ, M. N. (1981), *Elastic Wave Propagation in a Fluid-filled Borehole and Synthetic Acoustic Logs*, Geophysics 46, 1042–1053.
- COUTANT, O. (1989), *Numerical Study of the Diffraction of Elastic Waves by Fluid-filled Cracks*, J. Geophys. Res. 94, 17805–17818.
- DONG, W., BOUCHON, M., and TOKSÖZ, M. N. (1995), *Borehole Seismic-source Radiation in Layered Isotropic and Anisotropic Media: Boundary Element Modeling*, Geophysics 60, 735–747.
- GAFFET, S. (1995), *Teleseismic Wave Form Modeling Including Geometrical Effects of Superficial Geological Structures near to Seismic Sources*, Bull. Seismol. Soc. Am. 85, 1068–1079.
- GAFFET, S., and BOUCHON, M. (1989), *Effects of Two-dimensional Topographies Using the Discrete Wave Number—Boundary Integral Equation Method in P-SV Cases*, J. Acoust. Soc. Am. 85, 2277–2283.
- GAFFET, S., and BOUCHON, M. (1991), *Source Location and Valley Shape Effects on the P-SV Displacement Field Using a Boundary Integral Equation—Discrete Wave-number Representation Method*, Geophys. J. Int. 106, 341–355.
- GAFFET, S., MASSINON, B., PLANTET, J. L., and CANSI, Y. (1994), *Modelling Local Seismograms of French Nuclear Tests in Taouriri tan Afella Massif, Hoggar, Algeria*, Geophys. J. Int. 119, 964–974.
- GIBSON, R. L., and CAMPILLO, M. (1994), *Numerical Simulation of High- and Low-frequency Lg-wave Propagation*, Geophys. J. Int. 118, 47–56.
- HAARTSEN, M. W., BOUCHON, M., and TOKSÖZ, M. N. (1994), *A Study of Seismic Acoustic Wave Propagation through a Laterally-varying Multilayered Medium Using the Boundary-integral-equation—Discrete Wave-number Method*, J. Acoust. Soc. Am. 96, 3010–3021.
- KAWASE, H. (1988), *Time-domain Response of a Semicircular Canyon for Incident SV, P, and Rayleigh Waves Calculated by the Discrete Wave-number Boundary Element Method*, Bull. Seismol. Soc. Am. 78, 1415–1437.
- KAWASE, H., and AKI, K. (1989), *A Study of the Response of a Soft Basin for Incident S, P, and Rayleigh Waves with Special Reference to the Long Duration Observed in Mexico City*, Bull. Seismol. Soc. Am. 79, 1361–1382.
- KAWASE, H., and AKI, K. (1990), *Topography Effect at the Critical SV Wave Incidence: Possible Explanation of Damage Pattern by the Whittier Narrows, California, Earthquake of 1 October 1987*, Bull. Seismol. Soc. Am. 80, 1–22.
- KENNETT, B. L. N. (1974), *Reflections, Rays and Reverberations*, Bull. Seismol. Soc. Am. 65, 1643–1651.
- MAL, A. K. (1970), *Interaction of Elastic Waves with a Griffith Crack*, Int. J. Eng. Sci. 8, 763–776.
- MÜLLER, G. (1985), *The Reflectivity Method: A Tutorial*, J. Geophys. 58, 153–174.
- PAUL, A. (1994), *Synthetic Seismic Sections of a Lower Crust with Undulating Interfaces*, Annales Geophysicae 12, C61.
- PAUL, A., and CAMPILLO, M. (1988), *Diffraction and Conversion of Elastic Waves at a Corrugated Interface*, Geophysics 53, 1415–1424.

- PAUL, A., JONGMANS, D., CAMPILLO, M., MALIN, P., and BAUMONT, D. (1996), *Amplitudes of Regional Seismic Phases in Relation to the Crustal Structure of the Sierra Nevada (California)*, J. Geophys. Res. (in press).
- SHAPIRO, N., BÉTHOUX, N., CAMPILLO, M., and PAUL, A. (1996), *Regional Seismic Phases across the Ligurian Sea: Lg Blockage and Oceanic Propagation*, Phys. Earth and Planet. Inter. 93, 257–268.

(Received July 10, 1995, revised January 15, 1996, accepted February 27, 1996)